

TGF β signaling links early-life endocrine-disrupting chemicals exposure to suppression of nucleotide excision repair in rat myometrial stem cells

Maria Victoria Bariani

University of Chicago Department of Obstetrics and Gynecology

Yan-Hong Cui

University of Chicago Department of Medicine

Mohamed Ali

University of Chicago Department of Obstetrics and Gynecology

Tao Bai

University of Chicago Department of Obstetrics and Gynecology

Sandra L. Grimm

Baylor College of Medicine

Cristian Coarfa

Baylor College of Medicine

Cheryl L. Walker

Baylor College of Medicine

Yu-Ying He

University of Chicago Department of Medicine

Qiwei Yang

University of Chicago Department of Obstetrics and Gynecology

Ayman Al-Hendy (✉ aalhendy@bsd.uchicago.edu)


University of Chicago Department of Obstetrics and Gynecology <https://orcid.org/0000-0002-8778-4447>

Research Article

Keywords: Uterine fibroid risk, myometrial stem cells, endocrine-disrupting chemicals, transforming growth factor beta, nucleotide excision repair, developmental reprogramming

Posted Date: June 7th, 2023

DOI: <https://doi.org/10.21203/rs.3.rs-3001855/v1>

License:  This work is licensed under a Creative Commons Attribution 4.0 International License. [Read Full License](#)

Abstract

Environmental exposure to endocrine-disrupting chemicals (EDCs) is linked to the development of uterine fibroids (UFs) in women. UFs, non-cancerous tumors, are thought to originate from abnormal myometrial stem cells (MMSCs). Defective DNA repair capacity may contribute to the emergence of mutations that promote tumor growth. The multifunctional cytokine TGF β 1 is associated with UF progression and DNA damage repair pathways. To investigate the impact of EDC exposure on TGF β 1 and nucleotide excision repair (NER) pathways, we isolated MMSCs from 5-months old Eker rats exposed neonatally to Diethylstilbestrol (DES), an EDC, or to vehicle (VEH). EDC-MMSCs exhibited overactivated TGF β 1 signaling and reduced mRNA and protein levels of NER pathway components compared to VEH-MMSCs. EDC-MMSCs also demonstrated impaired NER capacity. Exposing VEH-MMSCs to TGF β 1 decreased NER capacity while inhibiting TGF β signaling in EDC-MMSCs restored it. RNA-seq analysis and further validation revealed decreased expression of Uvr α , a tumor suppressor gene involved in DNA damage recognition, in VEH-MMSCs treated with TGF β 1, but increased expression in EDC-MMSCs after TGF β signaling inhibition. Overall, we demonstrated that the overactivation of the TGF β pathway links early-life exposure to EDCs with impaired NER capacity, which would lead to increased genetic instability, arise of mutations, and fibroid tumorigenesis. We demonstrated that the overactivation of the TGF β pathway links early-life exposure to EDCs with impaired NER capacity, which would lead to increased fibroid incidence.

Introduction

The incidence of uterine fibroids (UFs) is extremely common among women of reproductive age. Although non-cancerous, these tumors are associated with significant morbidity, including prolonged or heavy menstrual bleeding, pelvic pain, and in some cases, they can be related to pregnancy loss and infertility [1]. Despite the last few years have shown emergence of different treatment alternatives, UFs continue to be the most common cause of hysterectomy, which in turn increases these women's risk for several medical complications [2].

Risk factors for the development of these tumors include race/ethnicity, age, parity, and Vitamin D deficiency [1]. Notably, endocrine-disrupting chemicals (EDCs), both natural and anthropogenic, are capable of disrupting the endocrine system, and may contribute to some of the most prevalent female reproductive disorders [3, 4]. In this sense, environmental EDCs exposure is considered an important risk factor for UF pathogenesis [5, 6]. Moreover, epidemiological studies have confirmed the correlation between early life exposure to EDCs and increased risk for early UF diagnosis [7–10]. However, to understand how the exposure to EDCs during critical uterine developmental period could increase the incidence of UFs is yet unclear and necessary to appeal to animal experimentation, and the best-characterized animal model for this is the Eker rat. These animals carry a defect in the *Tsc2* tumor suppressor gene and female Eker rats develop UFs spontaneously with a high frequency during their adulthood [11]. Cook et al. [12] have shown that early-life exposure to diethylstilbestrol (DES) during the development of the uterus increased *Tcs2* penetrance, tumor multiplicity and size, demonstrating that developmental exposure to EDCs can permanently reprogram tissue responses. Even though DES is not currently in use, it is an effective tool to study the effects induced by this EDC since many environmental xenoestrogens such as dibutyl phthalate (DBP) have a similar impact on reproductive health [13].

Several studies support the argument that UFs originate from transformed myometrial stem cells (MMSCs) [14–16]. DNA damage response and repair processes maintain the integrity of genomic DNA, and failures in these mechanisms may be the cause behind the transformation of a normal MMSC to a tumor initiating cell [17, 18]. In

this regard, EDCs can cause DNA damage upon exposure [19, 20]. Previous observations from our group have indicated that the expression of DNA repair-related genes/proteins is reprogrammed by early-life EDCs exposure in MMSCs isolated from adult Eker rats [21, 22]. Nucleotide excision repair (NER) is a highly conserved DNA repair pathway, capable of removing structurally bulky DNA helix distortion lesions from the genome, generated by chemicals or UV radiation [23, 24]. To date, there is limited available information regarding the potential inference of the NER pathway on the physiopathology of UF. A single report done in southern Chinese women has linked a higher susceptibility to UF with a single nucleotide polymorphism in *XPG* gene (rs873601 G > A), a crucial protein involved in NER repair processes [25].

Transforming growth factor β (TGF β) is a secreted cytokine that exists in mammals in three isoforms (TGF β 1, TGF β 2, and TGF β 3). TGF β controls a plethora of processes, such as apoptosis, angiogenesis, and tumor biology [26], and is considered one of the key factors in the pathophysiology of UFs [27]. Several studies have suggested a connection between TGF β signaling and DNA damage response [28, 29]. Previous analyses reported a link between TGF β 1 pathway and steroid hormone signaling [30, 31] or EDCs treatment [32, 33].

This work aimed to elucidate the role of both TGF β 1 and the NER, as well as their link to the tumorigenesis process on MMSCs, the cell origin of UFs, in the best-characterized animal model of UFs for gene-environment interaction.

Material and Methods

Animal model and Myometrial Stem Cell isolation and culture

Female Eker rats from an on-site colony (Long Evans; *TSC-2^{EK/+}*) received subcutaneous injections of 10 μ g of the endocrine-disrupting chemical (EDC) Diethylstilbestrol (DES, D4628, Sigma, St. Louis, MO, USA) per rat per day or 50 μ l of sesame seed oil (vehicle, VEH, S3547, Sigma, St. Louis, MO, USA) on 10, 11, and 12 postnatal days, a sensitive period for uterine developmental programming, as previously described [12]. Animals were euthanized at 5 months of age and subjected to myometrial Stro1+/CD44+ stem cell isolation, according to a previously described protocol [80]. Briefly, uterine tissues from Eker rat exposed to VEH (N = 5, pooled) or EDC (N = 5, pooled) were collected, washed to remove residual blood, and the endometrial and serosal tissues were removed by scraping with a sterile scalpel. Myometrial tissues were digested into single-cell suspensions, which were subjected to selection for Stro1/CD44 double-positivity by magnetic beads (mouse anti-Stro1, MAB1038, R&D Systems and mouse anti-CD44, #555478, BD Biosciences, respectively) to isolate Stro1+/CD44+ MMSCs. Then, isolated VEH- and EDC-MMSCs were plated in coated flasks (Attachment factor #S006100, Thermo Fisher Scientific, Waltham, MA) and cultured separately in Smooth Muscle Growth Medium-2 BulletKit (complete SmGm media) (CC-3182, Lonza, Walkersville, MD) under hypoxic conditions (37°C, 5% CO₂, 2% O₂). Confluent VEH- and EDC-MMSCs were washed with PBS, trypsinized (TrypLE Express Enzyme, 12604021, Thermo Fisher Scientific, Waltham, MA), and centrifuged at 500 \times g for 5 min. Supernatants were aspirated, and pellets were stored at -80°C until further use. Protocols involving the use of these animals were approved by the Institutional Animal Care & Use Committee (IACUC), Baylor College of Medicine (protocol # AN-7189).

RNA isolation, cDNA synthesis, and quantitative real-time PCR

Total cellular RNA was isolated from frozen MMSCs pellets using TRIzol Reagent (#15596026, Invitrogen, Waltham, MA, USA) following manufacturer instructions. RNA reverse transcription to complementary DNA

(cDNA) was performed using Ecody premix double-primed (#639549, Takara Bio, San Jose, CA, USA). Quantitative real-time PCR (qPCR) was carried out using SsoAdvanced Universal SYBR Green Supermix (Bio-Rad, Hercules, CA, USA) in a 20- μ L final reaction volume. Primer sequences are listed in Table 1. Primers were purchased from Integrated DNA Technologies (IDT, Coralville, IA, USA) excluding *Ltbp1*, *Tgfb1*, *Smad3*, and *Uvrag* primers (Product IDs: RQP050189, RQP050181, RQP090103, RQP083172, respectively) that were purchased from Genecopoeia (Rockville, MD, USA). Real-time PCR analyses were performed using the Bio-Rad CFX96 detection system (Bio-Rad, Hercules, CA, USA). A melting-curve analysis affirmed the synthesis of a DNA product of the predicted size. The expression data were normalized using *18S* ribosomal RNA values, and these relative normalized values were used to generate data graphs. A reaction without a cDNA template was used as a negative control.

Table 1
Rat primer sequences for RT-qPCR.

Symbol/Alias	Gene	Forward primer sequence (5'-3')	Reverse primer sequence (5'-3')
<i>Thbs-1</i>	Thrombospondin 1	TCGGGGCAGGAAGACTATGA	ACTGGGCAGGGTTGTAATGG
<i>Smad2</i>	Mothers against decapentaplegic homolog 2	GGGAAGTGTTTGCCGAGTG	AGCCTGGTGGGATTTTGC
<i>Xpa</i>	DNA damage recognition and repair factor	CAGACACCAGAGCCACTTTAC	GCAGACACCCATACACAATGA
<i>Xpb, Ercc3</i>	Xeroderma pigmentosum complementation group B, ERCC excision repair 3, TFIIH Core Complex Helicase Subunit	GGGTACTCAGAGCCAAGAAAG	GAATCTCTGTCGCTTGGTAGAA
<i>Xpc</i>	Xeroderma pigmentosum complementation group C	CACCTCCATCAGCACATACAA	ACAGCTTCTCCACGACAATAC
<i>Xpf, Ercc4</i>	Xeroderma pigmentosum complementation group F, ERCC Excision Repair 4, Endonuclease Catalytic Subunit	TAAGCTCACACTCCTCACCT	CCAGGGTTATACCTGTCTGA
<i>Xpd, Ercc2</i>	Xeroderma pigmentosum complementation group D, ERCC excision repair 2, TFIIH core complex helicase	TTACTACAGCGCAGAGCCAG	ACCCCAAACATTTCACCCACT
<i>Ddb1</i>	DNA damage-binding protein 1	CACGGTTCCTCTCTATGAATCTC	TAGTGCCTCCACTGGTATCT
<i>Ddb2</i>	DNA damage-binding protein 2	TGGTGGTTACAGGAGACAATATG	GCCACATGGGCTACTTTCT
<i>18S</i>	18S ribosomal RNA	CACGGACAGGATTGACAGATT	GAGTCTCGTTCGTTATCGGAATTA

Protein expression analysis by western blot

VEH- and EDC-MMSCs pellets were lysed in RIPA buffer (#89900, Thermo Fisher Scientific, Waltham, MA) containing 1% of protease and phosphatase Inhibitor Cocktail (#78440, Thermo Fisher Scientific, Waltham, MA), vortexed, sonicated, and centrifuged for 10 min at 12,000 RPM at 4°C. Three experimental replicates per group

were run. Samples equivalent to 25 µg of protein were separated using 4–20% Mini-PROTEAN TGX Precast Protein Gels (#4561096, Bio-Rad, Hercules, CA) and transferred to Trans-Blot Turbo Midi 0.2 µm PVDF membranes (#1704157, Bio-Rad, Hercules, CA) according to standard procedures. Membranes were blocked for 1 h at RT in either 5% w/v nonfat dry milk or 5% BSA in 0.1% Tween-supplemented PBS (0.1% PBS-T) per antibody specification. Membranes were then incubated with primary antibodies overnight at 4°C in either 1% w/v nonfat dry milk or 1% BSA in 0.1% PBS-T per antibody specification. Following is the information regarding the primary antibodies used, their source, and working dilutions: rabbit anti-LTBP1 (ab78294, Abcam; 1:1000), rabbit anti-THBS1 (MA5-13398, Invitrogen; 1:1000), rabbit anti-TGFβ 1 (MA5-15065, Invitrogen; 1:1000), rabbit anti-p-SMAD2 (Ser465/467) (#3108, Cell Signaling; 1:1000), rabbit anti-SMAD2 (#5339, Cell Signaling; 1:1000), rabbit anti-XPA (PA5-86265, Invitrogen; 1:1000), mouse anti-XPB (#8746, Cell Signaling; 1:1000), mouse anti-XPC (sc-74410, Santa Cruz; 1:1000), rabbit anti-XPD (#11963, Cell Signaling; 1:1000), rabbit anti-XPG (PA5-76039, Invitrogen; 1:1000), rabbit anti-XPF (#13465, Cell Signaling; 1:1000), rabbit anti-DDB1 (#5428, Cell Signaling; 1:1000), mouse anti-DDB2 (sc-81246, Santa Cruz; 1:1000). Mouse anti-β-Actin (A5441, Sigma, 1:10000) protein levels were assessed by re-probing the blots. Membranes were washed in 0.1% PBS-T and then incubated with anti-rabbit (#7074, Cell Signaling; 1:5000) or anti-mouse (#7076, Cell Signaling; 1:5000) horseradish peroxidase-labeled antibodies. The antigen–antibody complex was detected with Trident femto Western HRP Substrate kit (GTX14698, GeneTex, Irvine, CA, USA) and images of immunoreactive bands were acquired using ChemiDoc XRS + molecular imager (Bio-Rad, Hercules, CA, USA). Bands were analyzed using Image J software [81]. The relative protein level was normalized to β-actin and results were expressed as relative optical density.

Measurement of TGFβ1 levels in MMSCs culture supernatants

VEH- and EDC-MMSCs were cultured until confluence in previously stated conditions. Then, cells were washed thoroughly using PBS, and media were replenished with complete SmGm media without fetal bovine serum. MMSCs culture supernatant (CS) samples were collected after 6 h and frozen in aliquots at – 80°C. TGFβ1 levels were detected in CS using a solid phase ELISA kit (DB100C, R&D Systems, Minneapolis, MN, USA) according to the manufacturer's protocol.

Immunofluorescence

VEH- and EDC-MMSCs were seeded onto coated-glass coverslips and culture under the conditions stated above. Confluent cells were then fixed with 4% paraformaldehyde for 15 minutes, followed by permeabilization with 0.1% Triton X-100 in PBS for 15 minutes at room temperature. Non-specific binding was blocked with 2% BSA in PBS for 1 hour at room temperature. Primary antibody targeting TGFβ1 (MA5-15065, Invitrogen, 1:100 in 0.1% BSA-PBS) and TGFβ Receptor I (PA-95863, Invitrogen, 1:100 in 0.1% BSA-PBS) were applied and incubated overnight at 4°C. The cells were then washed with PBS three times for 5 min and incubated with Alexa Fluor™ 568-conjugated α-Rabbit secondary antibody (A11011, Invitrogen, 1:2000 in 0.1% BSA-PBS) for 1 hour at room temperature. Finally, the coverslips were mounted onto glass slides using mounting medium containing DAPI for nuclear counterstaining (H-1200, VECTASHIELD). Digital image files were created with an Olympus VS200 Research Slide Scanner (Olympus / Evident, Center Valley, PA) with a Hamamatsu ORca-Fusion camera (Hamamatsu Photonics, Skokie, IL). Individual images were created with the OlyVIA Viewer software (Olympus / Evident, Center Valley, PA). Negative controls without primary antibody were included to validate the staining specificity.

Immunohistochemistry

Myometrial tissue samples from 5 months old Eker rat exposed neonatally to VEH or EDC were fixed in 10% buffered formalin for 15–20 h and embedded with paraffin. Paraffin blocks were sliced into 5- μ M thick sections, deparaffinized with xylene, and rehydrated by being passed through decreasing concentrations of ethanol in water. Then, antigen retrieval and quenching of endogenous peroxidases were performed. The primary antibodies used to detect XPA and XPC were rabbit anti-XPA (PA5-86265, Invitrogen; 1:250) and mouse anti-XPC (sc-74410, Santa Cruz; 1:200), respectively. Samples were scanned and visualized using Aperio Image Scope Software (v12.4.0.7018) (Leica Biosystems Imaging Inc., Deer Park, IL, USA).

MMSCs TGF β 1 and TGF β Receptor I inhibitor treatments

Once VEH- or EDC-MMSCs reached 80% confluence, they were treated with human recombinant TGF β 1 (10 ng/ml, 7754-BH, R&D Systems,) for 48 h or with TGF β Receptor I inhibitor (2 μ M, LY-364947, L6293, Sigma, St. Louis, MO, USA) for 24 h, respectively. The vehicle used to dissolve TGF β 1 was 4 mM HCl (SA49, Thermo Fisher Scientific, Waltham, MA, USA) containing 0.1% bovine serum albumin (BSA, A3294, Sigma, St. Louis, MO, USA). Mature human TGF β 1 shares 99% amino acid identity with rat TGF β 1, and it demonstrated cross-species activity [82]. Dimethyl sulfoxide (DMSO, 472301, Sigma, St. Louis, MO, USA) was used as a VEH to dissolve the TGF β Receptor I inhibitor (final concentration < 0.1%). VEH- and EDC-treated MMSCs were washed with PBS, trypsinized, and centrifuged at 500 \times g for 5 min. The supernatant was discarded, and the pellets were snap-frozen and stored at -80°C for RNA isolation.

Determination of UVB-induced DNA damage in genomic DNA by slot blot assay

VEH- and EDC-MMSCs pellets were collected as described above at different time points (0, 6, and 12 h) post-UVB light exposure (10 mJ/cm²), and DNA was isolated using a QIAamp DNA Mini Kit (#51304, Qiagen, Valencia, CA). The DNA concentration was calculated from the absorbance at 260 nm using NanoDrop 1000 (NanoDrop products, Wilmington, DE). The cyclobutane pyrimidine dimers (CPD) in DNA were quantified by slot blot (Bio-Rad) with CPD monoclonal (TDM-2) antibody (CAC-NM-DND-001, COSMO BIO Co., Koto-Ku, Tokyo, Japan) as described previously [83]. The chemiluminescence was detected with a Carestream Imaging Station (Carestream, Rochester, NY, USA). For examining repair kinetics, the percentage (%) of CPD repair was calculated by comparing the optical density at the indicated time to that of the corresponding absorbance at time zero when there was no opportunity for repair, and 100% of CPDs were present post-UVB. The 10 mJ/cm² UVB dose was chosen as there was little acute, UV-induced cell death (observed under light bright microscopy) induced under these conditions, while there were sufficient levels of DNA damage to reproducibly measure its repair (doses between 10 ~ 30 mJ/cm² were screened initially).

Whole-genome RNA sequencing (RNA-seq)

RNA quality and quantity were assessed using the Agilent bio-analyzer. Strand-specific RNA-SEQ libraries were prepared using a TruSEQ mRNA-SEQ library protocol (Illumina provided). Library quality and quantity were assessed using the Agilent bio-analyzer, and libraries were sequenced using an Illumina NovaSEQ6000 (Illumina provided reagents and protocols). A variety of R packages were used for this analysis. All packages used are available from the Comprehensive R Archive Network (CRAN), Bioconductor.org, or Github. The reads were mapped to the *R. norvegicus* reference genome Rnor 6.0 using STAR 2.7.9a. Aligned reads were quantified using Salmon 1.4.0, and gene annotations from Ensembl were used to summarize data from transcript level to gene

level. We filtered non-protein coding genes as well as genes with less than 1 count per million in at least 3 or more samples and applied TMM normalization. To identify differentially expressed genes (DEGs), precision weights were applied to gene counts based on within-group sample-level variance and gene-level mean-variance trends using VOOM from Limma 3.52.4. The count data was fitted to a gene-wise linear model with group status as a coefficient, and an empirical Bayes method was used to estimate the posterior odds of differential expression after adjusting for gene-level posterior residual standard deviations. Significant differential genes were decided with a minimum absolute fold change of 1.5 and a false-discovery rate of 0.05. GSEA was tested using the Hallmark MSigDB collection.

Statistical analysis

Comparisons between groups were made by two-tailed unpaired Student's t-test using GraphPad Prism 9 (GraphPad Software, San Diego, CA). The assumption of normality was assessed by Shapiro–Wilks test. All data are presented as mean ± standard error of mean (S.E.M.). A difference between groups with * $p < 0.05$, ** $p < 0.005$, *** $p < 0.0005$, or **** $p < 0.0001$ was considered statistically significant.

Results

The TGFβ1 signaling pathway is overactivated in MMSCs isolated from rats exposed to EDCs

To identify transcriptional changes in the context of early-life EDCs exposure, we performed RNA-seq on MMSCs isolated from 5-months old Eker rats exposed neonatally to VEH or to diethylstilbestrol (DES), an EDC that mimic estrogen action [34]. We found 2922 DEGs (1474 up, and 1448 down) in EDC- over VEH-MMSCs (Figure S1 A). Among the DEGs, we found 14 genes belonging to TGFβ signaling (Figure S1 B). In addition, pathway analysis using Hallmark compendium showed significant enrichment of the HALLMARK_TGF_BETA_SIGNALING pathway (Figure S1 C). There is evidence that perinatal exposure to the estrogenic EDC methoxychlor reprogramed *Tgfb1* gene expression in the hypothalamus of Fischer rats [35]. Moreover, Cometti et al. have reported that certain environmental estrogen induced TGFβ1 levels in bovine oviduct cell culture [36], linking steroid hormone signaling with TGFβ1. In this study, to determine whether early life exposure to EDCs affected TGFβ1 pathway on rat MMSCs, we first analyzed several members of this superfamily. We found that the mRNA and protein levels of latent TGFβ binding protein 1 (LTBP1), which controls TGFβ1 bioavailability by maintaining it in a latent state in the extracellular matrix [37], were increased in EDC-MMSCs compared to VEH-MMSCs (Fig. 1A). Further, we observed the same outcome for thrombospondin-1 (TSP1), a major regulator of latent TGFβ1 activation [38] (Fig. 1B). We further confirmed that TGFβ1 mRNA and protein levels are also elevated in MMSCs isolated from rats exposed to EDCs in early life (Fig. 1C and E). Moreover, as illustrated in Fig. 1D, the levels of TGFβ1 were significantly higher in the culture supernatants from EDC-MMSCs compared to the ones from VEH-MMSCs. Additionally, we confirmed the presence of TGFβ Receptor I on VEH- and EDC-MMSCs using immunofluorescence staining (Fig. 1F). SMADs are the main transducers of the TGFβ superfamily signal from the cell surface to the nucleus [39]. We found that the mRNA and protein levels of SMAD2 and p-SMAD2, which is considered a marker of TGFβ signaling activation, are increased respectively in EDC-MMSCs compared to the control (Fig. 1G and H) while *Smad3* (Fig. 1G) mRNA levels did not change. Overall, these results show that the TGFβ1 pathway is overactivated in MMSCs isolated from rats developmentally exposed to EDCs.

Early life exposure to EDCs provokes changes in MMSC NER pathway members

The analysis of EDC- and VEH-MMSC RNA-seq data demonstrated significant enrichment of the HALLMARK_UV_RESPONSE pathways along with enrichment of other pathways related to DNA damage repair such as HALLMARK_G2M_CHECPOINT (Figure S1 C). Moreover, 6 genes involved in nucleotide excision repair (NER) pathway showed changes in their mRNA expression levels between EDC-MMSCs and VEH-MMSC (Figure S1 D). NER is the main pathway involved in repairing bulky DNA adducts formed by environmental carcinogenic sources such as UV light exposure or chemical agents [40]. DES, the EDC used in this work as a research tool, is metabolized to reactive intermediates that covalently bind to DNA and nuclear proteins forming adducts [41]. To examine whether the factors that execute NER are regulated in MMSCs by environmental EDC exposure, we evaluate the mRNA and protein levels (Fig. 2A and B, respectively) of several core enzymes involved in different steps during the NER process. The damage sensor XPC exhibited lower mRNA and protein levels in EDC-MMSCs contrasted with VEH-MMSCs. Interestingly, when we evaluated DDB1 and DDB2 (DNA damage-binding protein 1 and 2), which also play central roles in the damage recognition process, we found that DDB1 mRNA and protein levels increased in EDC-MMSCs compared to the control. In contrast, DDB2 (also known as XPE) showed decreased mRNA levels on MMSCs isolated from EDC-exposed rats compared to controls but we did not see any differences in its protein levels. A previous study from our group have demonstrated that the mRNA levels of *Xpa*, which functions as a scaffold to assemble other NER core factors around the DNA damage site [42], were significantly downregulated in EDC-MMSCs compared with VEH-MMSCs [22]. In this work, we showed that the protein levels of XPA presented the same outcome (Fig. 2B). The DNA helicase XPB showed decreased mRNA and protein levels in EDC- versus VEH-MMSCs. However, we did not find any difference in the DNA helicase XPD mRNA or protein levels. XPF provides the endonuclease activity in a heterodimer complex that is essential for repairing DNA damage [43]. We observed that XPF mRNA and protein levels decreased in EDC-MMSCs in comparison to VEH-MMSCs. In conclusion, these results demonstrate that early life exposure to EDCs provokes changes in several NER pathway members in rat MMSCs, mostly, decreasing their levels.

MMSCs present self-renewal and differentiation capacities which are critical for myometrial tissue homeostasis. To evaluate whether the observed changes in NER pathway members take place also at the tissue level, we performed XPA and XPC IHC in myometrial tissues collected from adult rats (pre-fibroid) exposed neonatally to VEH or EDC (Fig. 2C). We found that the levels of both markers were lower in the myometrium of EDC-exposed rats compared to controls, suggesting that differentiated myometrial cells maintain characteristics of the parent MMSCs.

EDC-MMSCs present decreased ability to repair DNA by NER

To determine whether early life exposure to EDCs affects NER repair capability in MMSCs, we assessed the repair kinetic of cyclobutane pyrimidine dimers (CPD) after UVB exposure in VEH- and EDC-MMSCs. Cells were irradiated with 10 mJ/cm² UVB light and the cellular morphology were monitored by phase contrast light microscopy before and 9,12 and 24 h after the exposure. Figure 3A illustrates that EDC-MMSCs revealed more cell death than VEH-MMSCs 9 h after UVB light exposure. Although at 24 h, VEH-MMSCs also presented death-related cell debris, the levels of cell debris were markedly enhanced in EDC-MMSCs. As expected, EDC-MMSCs presented a significantly decreased ability to repair the UVB-induced CPD compared with the control group at 6 h

(VEH-MMSCs: 23.7% ± 2.5 vs. EDC-MMSCs: 8.3% ± 4.7, $p < 0.05$) and 12 h after the UVB exposure (VEH-MMSCs: 76.3% ± 4.1 vs. EDC-MMSCs: 7.6% ± 15, $p < 0.05$) (Fig. 3B).

The transforming growth factor- β 1 (TGF β 1) pathway regulates NER in rat MMSCs

TGF β 1 signaling has been implicated in regulating NER in human immortalized keratinocytes (HaCaT) cells (Qiang et al., 2016), but the link between these two pathways has not been evaluated in MMSC. We hypothesized that TGF β 1 pathway activation will compromise NER-dependent DNA repair in the healthy MMSC while TGF β 1 signaling inhibition will revert NER impairment in EDC-MMSC. To verify this hypothesis, we treated VEH-MMSCs with exogenous TGF β 1 and we observed that this activation suppressed CPD repair at 6 h (VEH-MMSCs: 70.6% ± 2.9 vs. VEH-MMSCs + TGF β 1: 33.3% ± 11.4, $p < 0.05$) and at 12 h (VEH-MMSCs: 71.3% ± 2.1 vs. VEH-MMSCs + TGF β 1: 63.1% ± 1.2, $p < 0.05$) after UVB light exposure (Fig. 3C). In this sense, when we inhibited TGF β Receptor I on EDC-MMSCs we found that EDC-MMSCs recovered the capacity to repair CPD at 6 h (EDC-MMSCs: 25.9% ± 6.7 vs. EDC-MMSCs + TGF β RI inhibitor: 53.4% ± 7, $p < 0.05$) (Fig. 3D). This data implies that TGF β 1 pathway is involved in regulating NER pathways in rat MMSCs.

Uvr g gene expression is affected by TGF β 1 activation and inhibition on rat MMSCs

We performed RNA-seq analysis to further investigate the effect of TGF β 1 activation and inhibition in VEH and EDC-MMSCs, respectively. The principal component analysis indicated that samples clustered by group (Fig. 4A). A total of 3220 DEG were found in the comparison of VEH-MMSCs treated with vehicle or TGF β 1. On the other hand, we observed 1402 DEG in EDC-MMSCs treated with vehicle or TGF β Receptor I inhibitor (Fig. 4A). The heatmaps confirmed that samples were separated by treatment (Fig. 4B). Volcano plots in Fig. 4C illustrate the distribution of DEG in VEH-MMSCs treated with vehicle or TGF β 1 (top) and in EDC-MMSCs treated with vehicle or TGF β Receptor I inhibitor (bottom). Genes of interest involved in NER and TGF β 1 pathways are indicated in the volcano plots. Interestingly, we observed that *Xpa* and *Xpc*, two NER members that were downregulated in EDC- compared to VEH-MMSCs (Fig. 2), were also downregulated on VEH-MMSC after the treatment with exogenous TGF β 1 (Fig. 4C, top). In addition, the *Ddb1* gene, which showed increased mRNA and protein levels in EDC- compared to VEH-MMSCs (Fig. 2), presented the same outcome in TGF β 1-treated VEH-MMSCs compared to the control (Fig. 4C, top). However, *Xpf* (also known as *Erc1*) showed the opposite result, since its levels were decreased in EDC- compared to VEH-MMSCs (Fig. 2) but increased in VEH-MMSC after the TGF β 1 treatment (Fig. 4C, top). Regarding the effect of TGF β Receptor I inhibitor on EDC-MMSCs transcriptome, we observed that the treatment increased the levels of *Xpc* gene (Fig. 4C, bottom), which, as we mentioned above, were downregulated in EDC- compared to VEH-MMSCs (Fig. 2). It is important to highlight that, as expected, the treatment of EDC-MMSCs with TGF β Receptor I inhibitor downregulated several genes that belong to TGF β 1 signaling such as *Thbs1*, *Ltbp1*, *Tgfb1*, *Tgfbr1*, *Smad6* and *Smad7* (Fig. 4C, bottom). Furthermore, UV-radiation Resistance Associated Gene (*Uvr g*) expression was downregulated in VEH-MMSCs after the treatment with exogenous TGF β 1 and upregulated after TGF β Receptor I inhibition in EDC-MMSCs. *Uvr g* specifically interacts with DDB1, which together with DDB2, checks the whole genome for damage independently of transcriptional status [44]. We confirmed the results by qPCR (Fig. 4D), noting that *Uvr g* mRNA levels were decreased in EDC compared to VEH-MMSCs. Next, we analyzed the top enriched Hallmark gene sets in VEH-MMSCs treated with TGF β 1 versus vehicle (Fig. 5A) and EDC-MMSCs treated with TGF β Receptor I inhibitor or vehicle (Fig. 5B) by

gene set enrichment analysis (GSEA) using Hallmark biological processes. The most significant enriched pathway in VEH-MMSCs treated with TGF β 1 in comparison with vehicle was HALLMARK_MTORC1_SIGNALING (Fig. 5A, top) while in EDC-MMSCs treated with TGF β Receptor I inhibitor versus vehicle was HALLMARK_INTERFERON_GAMMA_RESPONSE (Fig. 5B, top). Interestingly, GSEA identified that HALLMARK_UV_RESPONSE_DN gene set were significantly altered in EDC-MMSCs after TGF β Receptor I inhibitor (Fig. 5B). Altogether, these results confirm the link that exists between TGF β 1 and NER pathways.

Discussion

Transforming growth factor beta (TGF β) is a multipotent cytokine that is involved in several pathological processes in many cell types. Misregulation of TGF β activity has been related to tumorigenesis [45], including the development of UFs [46]. Recent studies have identified a connection between EDCs and TGF β . Song et al. [47] have shown that bisphenol S (BPS), an industrial EDC, increases the mRNA and protein levels of TGF β in non-small cell lung cancer (NSCLC) cells, and that their upregulation mediates BPS-induced NSCLC cell migration. Interestingly, in 3D human uterine leiomyoma (ht-UtLM) spheroids, the treatment with tetrabromobisphenol A (TBBPA), a derivative of bisphenol A (BPA), were found to induce an upregulated expression of profibrotic genes and corresponding proteins associated with the TGF β pathway [32]. The previously mentioned studies focused on the direct effects of EDC exposure on TGF β signaling, but it is likely that both direct and developmental EDC exposure may be mediated through similar pathways. In this sense, BPA exposure in pregnant rats delayed bone development and reduced bone mass in female offspring, and these results were accompanied by downregulated TGF β signaling pathway in the bone tissue [48]. In contrast, maternal exposure to di-n-butyl phthalate (DBP), which induces renal fibrosis in adult rat offspring, is related to increased TGF β mRNA and protein levels in the kidneys of DBP-exposed compared to unexposed 18-months old offspring [49]. In this current work, we have observed that EDC-MMSCs presented increased mRNA and protein levels of LTBP1, THBS1, and TGF β 1, and higher secreted levels of TGF β 1 compared to VEH-MMSCs, concluding that developmental EDC exposure overactivated TGF β 1 pathway. In the study by Liu et al. [32], TBBPA treatment activated TGF β signaling through phosphorylation of TGF β R1 and downstream effectors SMAD2 and SMAD3 in a 3D ht-UtLM spheroid model. Similarly in our study, we have detected increased levels of SMAD2 phosphorylation confirming the downstream activation of TGF β pathway, which after oligomerization with SMAD4, binds the DNA to mediate transcriptional activation or repression of target genes [50].

Besides the capacity of the EDCs to mimic the action of endogenous hormones, they have also been reported to exert genotoxic and mutagenic effects [51, 52]. The exposure to EDCs *in utero* or during early life is associated with the progression of diseases later in life [53, 54]. Developmental periods present increased susceptibility to environmental stressors and these components become important risk factors for adverse health outcomes. In this sense, epidemiological studies have suggested associations between several EDCs and increased UF prevalence and severity [55–58]. In addition, experimental animal studies have shown evidence that early-life exposure to EDCs, such as DES or genistein, induces anatomic abnormalities in the reproductive tract, including uterine tumors [59, 60]. It is important to highlight that environmental exposure to EDCs also can reprogram the cell epigenome, resulting in gene expression changes [6].

Several studies have demonstrated the presence of MMSCs [61, 62], which are able to self-renew while producing daughter cells that differentiate, and are susceptible to reprogramming by EDC exposure. Evidence points out that EDC or their reactive intermediates can interact with DNA altering DNA bases and leading to DNA damage

[51, 63]. Among the most common DNA lesions, single- and double-strand breaks [64], oxidative damage [65] and DNA adducts formation [66, 67] have been reported. Moreover, EDC can act through epigenetic mechanisms by which DNA damage repair is altered. The incapacity to correctly repair the DNA damage provoked by these compounds can lead to mutations and consequently, cells undergo modifications resulting in tumorigenesis. Moreover, the accepted model for the development of UFs establishes that they originate from an abnormal MMSC that acquire a driver mutation in pivotal genes such as *TSC-2* in the Eker rat or *MED12* in women. In particular, the Eker rat (*TSC-2*^{Ek/+}), inactivation of the wild-type *TSC-2* allele commonly occurs by loss of heterozygosity (LOH, caused by direct deletion, deletion due to unbalanced rearrangements, etc.). However, other mechanisms such as point mutation have also been reported [68]. Here we showed that MMSCs isolated from Eker rats that were exposed in early life to DES, a potent EDC, presented lower nucleotide excision repair (NER) capacity compared to VEH-MMSCs. Importantly, defective NER causes the accumulation of point mutations and genomic instability [69]. Therefore, this impaired capacity to repair the DNA could lead to the loss of the wild-type *TSC-2* allele in EDC-MMSCs, which would trigger the development of uterine tumors at a higher frequency in EDC-exposed Eker rats than unexposed. We found that the observed decreased NER capacity could be related to lower mRNA and protein levels of several members of this pathway, such as XPC, an indispensable factor for the initial recognition of bulky DNA damage [70]. There is evidence that demonstrates that the availability and the activity of NER factors can be regulated by environmental factors. In this sense, Notch et al. [71] described a marked reduction in the expression of genes involved in the NER pathway, including XPC, in the livers of zebrafish exposed to the xenoestrogen 17- α -ethinylestradiol (EE2). This study expanded our previous findings showing that developmental EDC exposure decreased DNA end-joining ability [22], and impaired ability to repair DNA double-strand breaks (DSBs) by homologous recombination pathway [21] in rat MMSCs.

Furthermore, we showed that increased levels of TGF β 1 affected the repair of bulky DNA damage, through modulation of nucleotide excision repair (NER). Although contradictory, several works showed a connection between TGF β 1 and DNA damage. While some authors showed that the inhibition of TGF β pathway tends to mitigate DNA damage responses and increase genomic instability [72–74], others demonstrated a possible role of activated TGF β signaling in reducing the expression and/or activity of some genes involved in DNA repair [29, 75, 76]. Regarding TGF β 1 and NER pathway, Qiang et al. [29] have shown that the activation of the TGF β pathway impairs UV-induced DNA repair by suppressing the transcription of XPC and DDB1. Additionally, we demonstrated that the treatment of VEH-MMSCs with exogenous TGF β 1 led to a decreased repair of DNA damage formed by ultraviolet-B radiation; a comparable response to that observed in EDC-MMSCs, which constitutively present activated endogenous TGF β 1 signaling. In accordance with this, we have shown that EDC-MMSCs treated with TGF β RI inhibitor recover the capacity to repair the DNA damage after 6h of UVB light exposure. Furthermore, we use RNA-seq data to identify NER-related genes that are affected by activation or inhibition of TGF β pathway in MMSCs. In particular, we discovered that TGF β signaling regulates the expression of genes such as *UVRAG*, which is essential in the NER pathway.

EDC exposure may be one factor driving the observed disparities in UF burden between Black and White women [77], as studies suggest that exposure to certain environmental EDC is higher in non-whites populations [78]. In this sense, a systematic review published by Ruiz et al. affirms that Black, Latinos, and low-income individuals have greater exposure rates to EDCs, such as certain phthalates, BPA, polychlorinated biphenyls, and organochlorine pesticides, than any other ethnic and sociodemographic population groups [79]. Importantly, it is

essential to recognize modifiable sources of EDC exposure that bring opportunities for reduction in racial/ethnic health disparities.

In summary, our findings pinpoint a link between the overactivation of TGF β and the impaired ability of rat MMSCs to repair DNA damage through the NER pathway, and both provoked by the developmental exposition to EDC, which have implications for uterine tumor development (Fig. 6).

Declarations

Acknowledgements

This work was supported by National Institutes of Health grants RO1 HD094378, RO1 ES028615, and U54 MD007602. We thank The University of Chicago Genomics Facility (RRID:SCR_019196) especially Pieter W. Faber, for their assistance with Illumina RNA sequencing. This work was supported in part through the computational resources and staff expertise provided by Evan Wu and Wenjun Kang from the Center for Research Informatics at The University of Chicago. We thank The University of Chicago Human Tissue Resource Center (RRID:SCR_019199), especially Dr. Terri Li and Dr. Can Gong for their assistance with immunohistochemistry services.

Funding

This work was supported by National Institutes of Health grants RO1 HD094378, RO1 ES028615, and U54 MD007602.

Competing Interests

The authors declare that they have no known competing financial interests or personal relationships that could have appeared to influence the work reported in this paper.

Authors' contributions

MVB made the major contribution to the acquisition, analysis, and interpretation of the data, and drafted the manuscript. YHC performed CPD slot blot, analyzed it and interpreted the data. MA cultured rat MMSC, performed TGF β 1 western blot, analyzed it and interpreted the data. TB cultured rat MMSC. SLG and CC analyzed VEH and EDC-MMSCs transcriptomic data. CLW supplied the Eker rats and performed DES exposures. QY and AAH contributed to the concept and design of the article. YYH, QY, and AAH revised the manuscript critically for important intellectual content. All authors read and approved the final manuscript.

Data availability

The datasets (Raw FASTQ files) generated during and/or analyzed during the current study are available in the NCBI Gene Expression Omnibus database with accession number GSE157503 (Supplementary Figure 1 - VEH-MMSC and EDC-MMSC) and GSE225636 (Figures 4 and 5- VEH-MMSC, VEH-MMSC + TGF β 1, EDC-MMSC, and EDC-MMSCs + TGF β RI inhibitor).

Ethics approval

All animal experiments were conducted in accordance with the policies and procedures set by the Institutional Animal Care & Use Committee (IACUC), Baylor College of Medicine (protocol # AN-7189).

Consent to participate

Not applicable.

Consent for publication

Not applicable.

References

1. Yang Q, Ciebiera M, Bariani MV et al (2022) Comprehensive Review of Uterine Fibroids: Developmental Origin, Pathogenesis, and Treatment. *Endocr Rev* 43:678–719. <https://doi.org/10.1210/edrv/bnab039>
2. Cohen SL, Vitonis AF, Einarsson JI (2014) Updated Hysterectomy Surveillance and Factors Associated With Minimally Invasive Hysterectomy. *JSL J Soc Laparoendosc Surg* 18. <https://doi.org/10.4293/JSL.2014.00096>. :e2014.00096
3. Padmanabhan V, Song W, Puttabyatappa M (2021) Praegnatio Perturbatio—Impact of Endocrine-Disrupting Chemicals. *Endocr Rev* 42:295–353. <https://doi.org/10.1210/edrv/bnaa035>
4. Crain DA, Janssen SJ, Edwards TM et al (2008) Female reproductive disorders: the roles of endocrine-disrupting compounds and developmental timing. *Fertil Steril* 90:911–940. <https://doi.org/10.1016/j.fertnstert.2008.08.067>
5. Bariani MV, Rangaswamy R, Siblini H et al (2020) The role of endocrine-disrupting chemicals in uterine fibroid pathogenesis. *Curr Opin Endocrinol Diabetes Obes* 27:380–387. <https://doi.org/10.1097/MED.0000000000000578>
6. Yang Q, Diamond MP, Al-Hendy A (2016) Early Life Adverse Environmental Exposures Increase the Risk of Uterine Fibroid Development: Role of Epigenetic Regulation. *Front Pharmacol* 7. <https://doi.org/10.3389/fphar.2016.00040>
7. D'Aloisio AA, Baird DD, DeRoo LA, Sandler DP (2010) Association of Intrauterine and Early-Life Exposures with Diagnosis of Uterine Leiomyomata by 35 Years of Age in the Sister Study. *Environ Health Perspect* 118:375–381. <https://doi.org/10.1289/ehp.0901423>
8. Omwandho COA, Konrad L, Halis G et al (2010) Role of TGF- β s in normal human endometrium and endometriosis. *Hum Reprod* 25:101–109. <https://doi.org/10.1093/humrep/dep382>
9. D'Aloisio AA, Baird DD, DeRoo LA, Sandler DP (2012) Early-Life Exposures and Early-Onset Uterine Leiomyomata in Black Women in the Sister Study. *Environ Health Perspect* 120:406–412. <https://doi.org/10.1289/ehp.1103620>
10. Baird DD, Newbold R (2005) Prenatal diethylstilbestrol (DES) exposure is associated with uterine leiomyoma development. *Reprod Toxicol* 20:81–84. <https://doi.org/10.1016/j.reprotox.2005.01.002>
11. Walker CL, Hunter D, Everitt JI (2003) Uterine leiomyoma in the Eker rat: A unique model for important diseases of women. *Genes Chromosom Cancer* 38:349–356. <https://doi.org/10.1002/gcc.10281>

12. Cook JD, Davis BJ, Cai S-L et al (2005) Interaction between genetic susceptibility and early-life environmental exposure determines tumor-suppressor-gene penetrance. *Proc Natl Acad Sci* 102:8644–8649. <https://doi.org/10.1073/pnas.0503218102>
13. Hunter D, Heng K, Mann N et al (2021) Maternal Exposure to Dibutyl Phthalate (DBP) or Diethylstilbestrol (DES) Leads to Long-Term Changes in Hypothalamic Gene Expression and Sexual Behavior. *Int J Mol Sci* 22:4163. <https://doi.org/10.3390/ijms22084163>
14. Mas A, Cervelló I, Gil-Sanchis C et al (2012) Identification and characterization of the human leiomyoma side population as putative tumor-initiating cells. *Fertil Steril* 98:741–751e6. <https://doi.org/10.1016/j.fertnstert.2012.04.044>
15. Ono M, Maruyama T, Masuda H et al (2007) Side population in human uterine myometrium displays phenotypic and functional characteristics of myometrial stem cells. *Proc Natl Acad Sci* 104:18700–18705. <https://doi.org/10.1073/pnas.0704472104>
16. Chang HL, Senaratne TN, Zhang L et al (2010) Uterine Leiomyomas Exhibit Fewer Stem/Progenitor Cell Characteristics When Compared With Corresponding Normal Myometrium. *Reprod Sci* 17:158–167. <https://doi.org/10.1177/1933719109348924>
17. Elkafas H, Qiwei Y, Al-Hendy A (2017) Origin of Uterine Fibroids: Conversion of Myometrial Stem Cells to Tumor-Initiating Cells. *Semin Reprod Med* 35:481–486. <https://doi.org/10.1055/s-0037-1607205>
18. Mani C, Reddy PH, Palle K (2020) DNA repair fidelity in stem cell maintenance, health, and disease. *Biochim Biophys Acta - Mol Basis Dis* 1866:165444. <https://doi.org/10.1016/j.bbadis.2019.03.017>
19. Iso T, Watanabe T, Iwamoto T et al (2006) DNA Damage Caused by Bisphenol A and Estradiol through Estrogenic Activity. *Biol Pharm Bull* 29:206–210. <https://doi.org/10.1248/bpb.29.206>
20. Xin F, Jiang L, Liu X et al (2014) Bisphenol A induces oxidative stress-associated DNA damage in INS-1 cells. *Mutat Res Toxicol Environ Mutagen* 769:29–33. <https://doi.org/10.1016/j.mrgentox.2014.04.019>
21. Elkafas H, Ali M, Elmorsy E et al (2020) Vitamin D3 Ameliorates DNA Damage Caused by Developmental Exposure to Endocrine Disruptors in the Uterine Myometrial Stem Cells of Eker Rats. *Cells* 9:1459. <https://doi.org/10.3390/cells9061459>
22. Prusinski Fernung LE, Yang Q, Sakamuro D et al (2018) Endocrine disruptor exposure during development increases incidence of uterine fibroids by altering DNA repair in myometrial stem cells†. *Biol Reprod*. <https://doi.org/10.1093/biolre/i0y097>
23. Kusakabe M, Onishi Y, Tada H et al (2019) Mechanism and regulation of DNA damage recognition in nucleotide excision repair. *Genes Environ* 41:2. <https://doi.org/10.1186/s41021-019-0119-6>
24. Cleaver JE, Lam ET, Revet I (2009) Disorders of nucleotide excision repair: the genetic and molecular basis of heterogeneity. *Nat Rev Genet* 10:756–768. <https://doi.org/10.1038/nrg2663>
25. Prud'homme GJ (2007) Pathobiology of transforming growth factor β in cancer, fibrosis and immunologic disease, and therapeutic considerations. *Lab Invest* 87:1077–1091. <https://doi.org/10.1038/labinvest.3700669>
26. Ciebiera M, Włodarczyk M, Wrzosek M et al (2017) Role of Transforming Growth Factor β in Uterine Fibroid Biology. *Int J Mol Sci* 18:2435. <https://doi.org/10.3390/ijms18112435>
27. Liu Q, Lopez K, Murnane J et al (2019) Misrepair in Context: TGF β Regulation of DNA Repair. *Front Oncol* 9. <https://doi.org/10.3389/fonc.2019.00799>

28. Qiang L, Shah P, Barcellos-Hoff MH, He YY (2016) TGF- β signaling links E-cadherin loss to suppression of nucleotide excision repair. *Oncogene* 35:3293–3302. <https://doi.org/10.1038/onc.2015.390>
29. Matsuda T, Yamamoto T, Muraguchi A, Saatcioglu F (2001) Cross-talk between Transforming Growth Factor- β and Estrogen Receptor Signaling through Smad3. *J Biol Chem* 276:42908–42914. <https://doi.org/10.1074/jbc.M105316200>
30. Kang H-Y, Lin H-K, Hu Y-C et al (2001) From transforming growth factor- β signaling to androgen action: Identification of Smad3 as an androgen receptor coregulator in prostate cancer cells. *Proc Natl Acad Sci* 98:3018–3023. <https://doi.org/10.1073/pnas.061305498>
31. Liu J, Yu L, Castro L et al (2022) Short-term tetrabromobisphenol A exposure promotes fibrosis of human uterine fibroid cells in a 3D culture system through TGF-beta signaling. *FASEB J* 36. <https://doi.org/10.1096/fj.202101262R>
32. Park M-A, Choi K-C (2014) Effects of 4-Nonylphenol and Bisphenol A on Stimulation of Cell Growth via Disruption of the Transforming Growth Factor- β Signaling Pathway in Ovarian Cancer Models. *Chem Res Toxicol* 27:119–128. <https://doi.org/10.1021/tx400365z>
33. Korach KS, Metzler M, McLachlan JA (1978) Estrogenic activity in vivo and in vitro of some diethylstilbestrol metabolites and analogs. *Proc Natl Acad Sci* 75:468–471. <https://doi.org/10.1073/pnas.75.1.468>
34. Gore AC, Walker DM, Zama AM et al (2011) Early Life Exposure to Endocrine-Disrupting Chemicals Causes Lifelong Molecular Reprogramming of the Hypothalamus and Premature Reproductive Aging. *Mol Endocrinol* 25:2157–2168. <https://doi.org/10.1210/me.2011-1210>
35. Cometti BPS, Dubey RK, Imthurn B, Rosselli M (2018) Natural and environmental oestrogens induce TGFB1 synthesis in oviduct cells. *Reproduction* 155:233–244. <https://doi.org/10.1530/REP-17-0425>
36. Robertson IB, Horiguchi M, Zilberberg L et al (2015) Latent TGF- β -binding proteins. *Matrix Biol* 47:44–53. <https://doi.org/10.1016/j.matbio.2015.05.005>
37. Murphy-Ullrich JE, Suto MJ (2018) Thrombospondin-1 regulation of latent TGF- β activation: A therapeutic target for fibrotic disease. *Matrix Biol* 68–69:28–43. <https://doi.org/10.1016/j.matbio.2017.12.009>
38. Witkowska M, Smolewski P (2014) SMAD family proteins: the current knowledge on their expression and potential role in neoplastic diseases. *Postepy Hig Med Dosw* 68:301–309. <https://doi.org/10.5604/17322693.1094726>
39. Cleaver JE (2005) Cancer in xeroderma pigmentosum and related disorders of DNA repair. *Nat Rev Cancer* 5:564–573. <https://doi.org/10.1038/nrc1652>
40. Green M, Wilson C, Newell O et al (2005) Diallyl sulfide inhibits diethylstilbesterol-induced DNA adducts in the breast of female ACI rats. *Food Chem Toxicol* 43:1323–1331. <https://doi.org/10.1016/j.fct.2005.02.005>
41. Borszéková Pulzová L, Ward TA, Chovanec M (2020) XPA: DNA Repair Protein of Significant Clinical Importance. *Int J Mol Sci* 21:2182. <https://doi.org/10.3390/ijms21062182>
42. Faridounnia M, Folkers G, Boelens R (2018) Function and Interactions of ERCC1-XPF in DNA Damage Response. *Molecules* 23:3205. <https://doi.org/10.3390/molecules23123205>
43. Gomes L, Menck C, Leandro G (2017) Autophagy Roles in the Modulation of DNA Repair Pathways. *Int J Mol Sci* 18:2351. <https://doi.org/10.3390/ijms18112351>
44. Baba AB, Rah B, Bhat GR et al (2022) Transforming Growth Factor-Beta (TGF- β) Signaling in Cancer-A Betrayal Within. *Front Pharmacol* 13:791272. <https://doi.org/10.3389/fphar.2022.791272>

45. Ciebiera M, Włodarczyk M, Wrzosek M et al (2017) Role of Transforming Growth Factor β in Uterine Fibroid Biology. *Int J Mol Sci* 18:2435. <https://doi.org/10.3390/ijms18112435>
46. Song P, Fan K, Tian X, Wen J (2019) Bisphenol S (BPS) triggers the migration of human non-small cell lung cancer cells via upregulation of TGF- β . *Toxicol Vitro* 54:224–231. <https://doi.org/10.1016/j.tiv.2018.10.005>
47. Wang T, Xu F, Song L et al (2021) Bisphenol A exposure prenatally delays bone development and bone mass accumulation in female rat offspring via the ER β /HDAC5/TGF β signaling pathway. *Toxicology* 458:152830. <https://doi.org/10.1016/j.tox.2021.152830>
48. Zhu Y-P, Chen L, Wang X-J et al (2017) Maternal exposure to di-n-butyl phthalate (DBP) induces renal fibrosis in adult rat offspring. *Oncotarget* 8:31101–31111. <https://doi.org/10.18632/oncotarget.16088>
49. Hata A, Chen Y-G (2016) TGF- β Signaling from Receptors to Smads. *Cold Spring Harb Perspect Biol* 8:a022061. <https://doi.org/10.1101/cshperspect.a022061>
50. Gwinn MR, Johns DO, Bateson TF, Guyton KZ (2011) A review of the genotoxicity of 1,2-dichloroethane (EDC). *Mutat Res Mutat Res* 727:42–53. <https://doi.org/10.1016/j.mrrev.2011.01.001>
51. Hercog K, Maisanaba S, Filipič M et al (2019) Genotoxic activity of bisphenol A and its analogues bisphenol S, bisphenol F and bisphenol AF and their mixtures in human hepatocellular carcinoma (HepG2) cells. *Sci Total Environ* 687:267–276. <https://doi.org/10.1016/j.scitotenv.2019.05.486>
52. Heindel JJ, Balbus J, Birnbaum L et al (2015) Developmental Origins of Health and Disease: Integrating Environmental Influences. *Endocrinology* 156:3416–3421. <https://doi.org/10.1210/en.2015-1394>
53. Hoover RN, Hyer M, Pfeiffer RM et al (2011) Adverse Health Outcomes in Women Exposed In Utero to Diethylstilbestrol. *N Engl J Med* 365:1304–1314. <https://doi.org/10.1056/NEJMoa1013961>
54. Zota AR, Geller RJ, Calafat AM et al (2019) Phthalates exposure and uterine fibroid burden among women undergoing surgical treatment for fibroids: a preliminary study. *Fertil Steril* 111:112–121. <https://doi.org/10.1016/j.fertnstert.2018.09.009>
55. Zota AR, Geller RJ, VanNoy BN et al (2020) Phthalate Exposures and MicroRNA Expression in Uterine Fibroids: The FORGE Study. *Epigenetics Insights* 13:251686572090405. <https://doi.org/10.1177/2516865720904057>
56. Lee J, Jeong Y, Mok S et al (2020) Associations of exposure to phthalates and environmental phenols with gynecological disorders. *Reprod Toxicol* 95:19–28. <https://doi.org/10.1016/j.reprotox.2020.04.076>
57. Lee G, Kim S, Bastiaansen M et al (2020) Exposure to organophosphate esters, phthalates, and alternative plasticizers in association with uterine fibroids. *Environ Res* 189:109874. <https://doi.org/10.1016/j.envres.2020.109874>
58. DeAnn Cook J, Davis BJ, Goewey JA et al (2007) Identification of a Sensitive Period for Developmental Programming That Increases Risk for Uterine Leiomyoma in Eker Rats. *Reprod Sci* 14:121–136. <https://doi.org/10.1177/1933719106298401>
59. Greathouse KL, Bredfeldt T, Everitt JI et al (2012) Environmental Estrogens Differentially Engage the Histone Methyltransferase EZH2 to Increase Risk of Uterine Tumorigenesis. *Mol Cancer Res* 10:546–557. <https://doi.org/10.1158/1541-7786.MCR-11-0605>
60. Mas A, Nair S, Laknaur A et al (2015) Stro-1/CD44 as putative human myometrial and fibroid stem cell markers. *Fertil Steril* 104:225–234e3. <https://doi.org/10.1016/j.fertnstert.2015.04.021>

61. Ono M, Bulun SE, Maruyama T (2014) Tissue-Specific Stem Cells in the Myometrium and Tumor-Initiating Cells in Leiomyoma1. <https://doi.org/10.1095/biolreprod.114.123794>. Biol Reprod 91:
62. Sicińska P, Mokra K, Wozniak K et al (2021) Genotoxic risk assessment and mechanism of DNA damage induced by phthalates and their metabolites in human peripheral blood mononuclear cells. Sci Rep 11:1658. <https://doi.org/10.1038/s41598-020-79932-5>
63. Vincent-Hubert F, Revel M, Garric J (2012) DNA strand breaks detected in embryos of the adult snails, *Potamopyrgus antipodarum*, and in neonates exposed to genotoxic chemicals. Aquat Toxicol 122–123:1–8. <https://doi.org/10.1016/j.aquatox.2012.05.004>
64. Franken C, Koppen G, Lambrechts N et al (2017) Environmental exposure to human carcinogens in teenagers and the association with DNA damage. Environ Res 152:165–174. <https://doi.org/10.1016/j.envres.2016.10.012>
65. Zhao H, Wei J, Xiang L, Cai Z (2018) Mass spectrometry investigation of DNA adduct formation from bisphenol A quinone metabolite and MCF-7 cell DNA. Talanta 182:583–589. <https://doi.org/10.1016/j.talanta.2018.02.037>
66. Saeed M, Rogan E, Cavalieri E (2009) Mechanism of metabolic activation and DNA adduct formation by the human carcinogen diethylstilbestrol: The defining link to natural estrogens. Int J Cancer 124:1276–1284. <https://doi.org/10.1002/ijc.24113>
67. Cook J, Walker C (2004) The Eker Rat: Establishing a Genetic Paradigm Linking Renal Cell Carcinoma and Uterine Leiomyoma. Curr Mol Med 4:813–824. <https://doi.org/10.2174/1566524043359656>
68. Gerasymchuk M (2021) Genomic instability and aging: Causes and consequences. Genome Stability: From Virus to Human Application. Elsevier Inc., pp 533–553
69. Shah P, He Y-Y (2015) Molecular Regulation of UV-Induced DNA Repair. Photochem Photobiol 91:254–264. <https://doi.org/10.1111/php.12406>
70. Notch EG, Miniutti DM, Mayer GD (2007) 17 α -Ethinylestradiol decreases expression of multiple hepatic nucleotide excision repair genes in zebrafish (*Danio rerio*). Aquat Toxicol 84:301–309. <https://doi.org/10.1016/j.aquatox.2007.06.006>
71. Kirshner J, Jobling MF, Pajares MJ et al (2006) Inhibition of Transforming Growth Factor- β 1 Signaling Attenuates Ataxia Telangiectasia Mutated Activity in Response to Genotoxic Stress. Cancer Res 66:10861–10869. <https://doi.org/10.1158/0008-5472.CAN-06-2565>
72. Glick AB, Weinberg WC, Wu IH et al (1996) Transforming growth factor beta 1 suppresses genomic instability independent of a G1 arrest, p53, and Rb. Cancer Res 56:3645–3650
73. Maxwell CA, Fleisch MC, Costes SV et al (2008) Targeted and Nontargeted Effects of Ionizing Radiation That Impact Genomic Instability. Cancer Res 68:8304–8311. <https://doi.org/10.1158/0008-5472.CAN-08-1212>
74. Pal D, Pertot A, Shirole NH et al (2017) TGF- β reduces DNA ds-break repair mechanisms to heighten genetic diversity and adaptability of CD44+/CD24 – cancer cells. <https://doi.org/10.7554/eLife.21615>. Elife 6:
75. Liu L, Zhou W, Cheng C-T et al (2014) TGF β Induces “BRCAness” and Sensitivity to PARP Inhibition in Breast Cancer by Regulating DNA-Repair Genes. Mol Cancer Res 12:1597–1609. <https://doi.org/10.1158/1541-7786.MCR-14-0201>
76. Eltoukhi HM, Modi MN, Weston M et al (2014) The health disparities of uterine fibroid tumors for African American women: a public health issue. Am J Obstet Gynecol 210:194–199.

<https://doi.org/10.1016/j.ajog.2013.08.008>

77. James-Todd TM, Chiu Y-H, Zota AR (2016) Racial/Ethnic Disparities in Environmental Endocrine Disrupting Chemicals and Women's Reproductive Health Outcomes: Epidemiological Examples Across the Life Course. *Curr Epidemiol Reports* 3:161–180. <https://doi.org/10.1007/s40471-016-0073-9>
78. Ruiz D, Becerra M, Jagai JS et al (2018) Disparities in Environmental Exposures to Endocrine-Disrupting Chemicals and Diabetes Risk in Vulnerable Populations. *Diabetes Care* 41:193–205. <https://doi.org/10.2337/dc16-2765>
79. Mas A, Stone L, O'Connor PM et al (2017) Developmental Exposure to Endocrine Disruptors Expands Murine Myometrial Stem Cell Compartment as a Prerequisite to Leiomyoma Tumorigenesis. *Stem Cells* 35:666–678. <https://doi.org/10.1002/stem.2519>
80. Schneider CA, Rasband WS, Eliceiri KW (2012) NIH Image to ImageJ: 25 years of image analysis. *Nat Methods* 9:671–675. <https://doi.org/10.1038/nmeth.2089>
81. Derynck Rik & Miyazono Kohei (2008) TGF- β and the TGF- β Family. *Cold Spring Harb Monogr Arch* 50
82. Nichols AF (2003) Basal transcriptional regulation of human damage-specific DNA-binding protein genes DDB1 and DDB2 by Sp1, E2F, N-myc and NF1 elements. *Nucleic Acids Res* 31:562–569. <https://doi.org/10.1093/nar/gkg152>

Figures

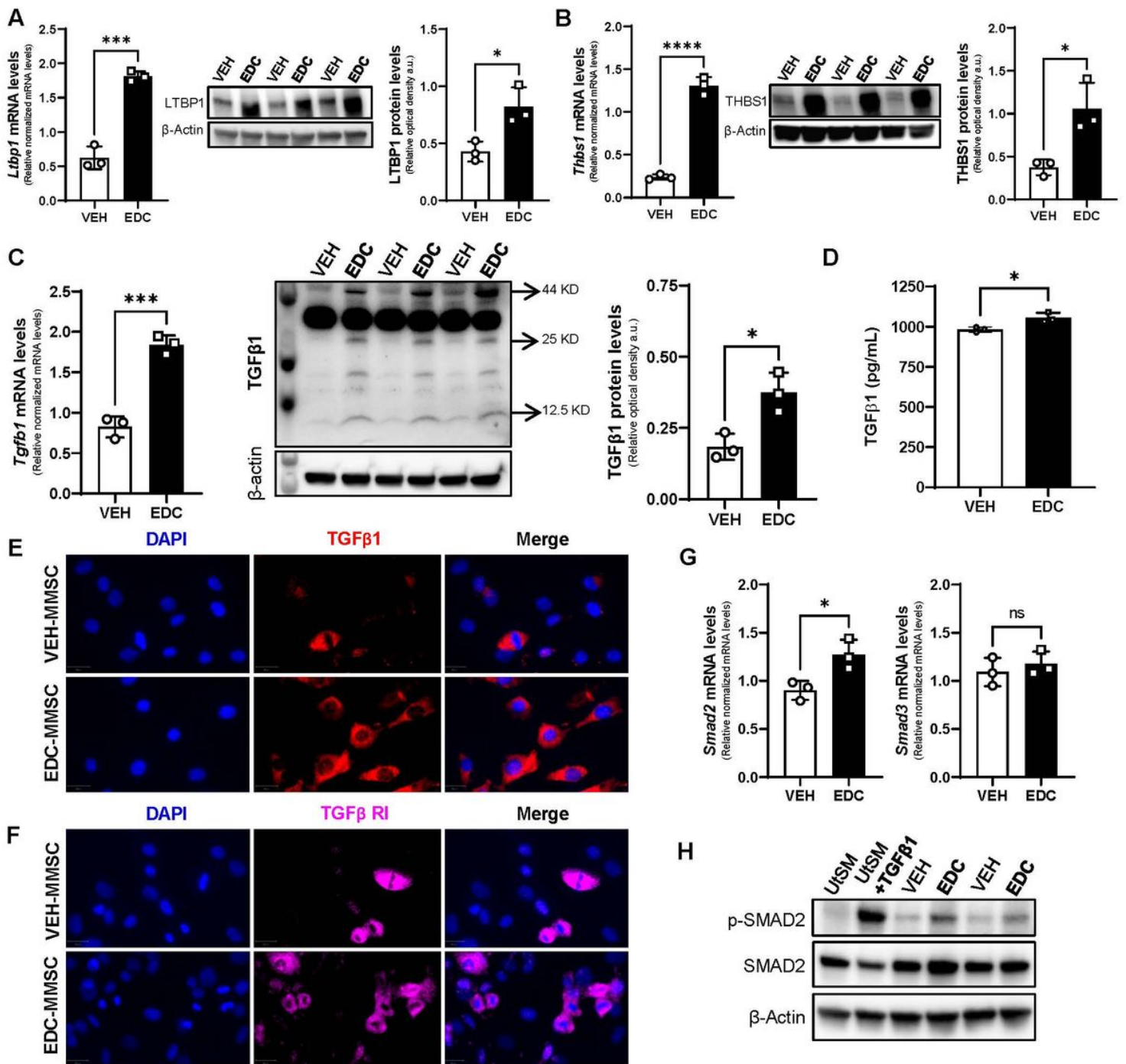


Figure 1

The TGFβ1 pathway is overactivated in MMSCs isolated from rats neonatally exposed to EDC. Real-time PCR analysis of mRNAs, protein levels and representative gels of **A**) LTBP1, **B**) THBS1, and **C**) TGFβ1 (arrows indicate band for: Pro-TGFβ1 at 44 kDa, Dimer of mature TGFβ1 at 25kDa, and Monomer of mature TGFβ1 at 12.5kDa) in VEH- and EDC-MMSCs isolated from 5-months old rats. **E**) TGFβ1 levels in culture supernatants collected from VEH- and EDC-MMSCs cultures. Immunofluorescence images of **D**) TGFβ1 and **F**) TGFβ1 RI in VEH- and EDC-MMSCs. Scale bar= 20 μm. **F**) mRNAs levels of *Smad2*, and *Smad3* in VEH- and EDC-MMSCs isolated from 5-months old rats. **G**) Representative gel of p-Smad2 and Smad2 in VEH- and EDC-MMSCs. mRNA data were normalized by the amount of 18S and protein levels by the amount of β-Actin. Data are shown as mean ± S.E.M.

from triplicate data. ns= not significant. *= p< 0.05, ***= p< 0.001, ****= p<0.0001, Student's t-test. EDC: endocrine disrupting chemical, MMSCs: myometrial stem cells, THBS1: Thrombospondin 1; LTBP1: Latent TGFβ binding protein 1. TGFβ1: Transforming growth factor beta 1. TGFβ RI: Transforming growth factor beta receptor 1. UtSM: human uterine smooth muscle cell line. TGFβ1 treatment: 10 ng/ml for 1h (positive control)

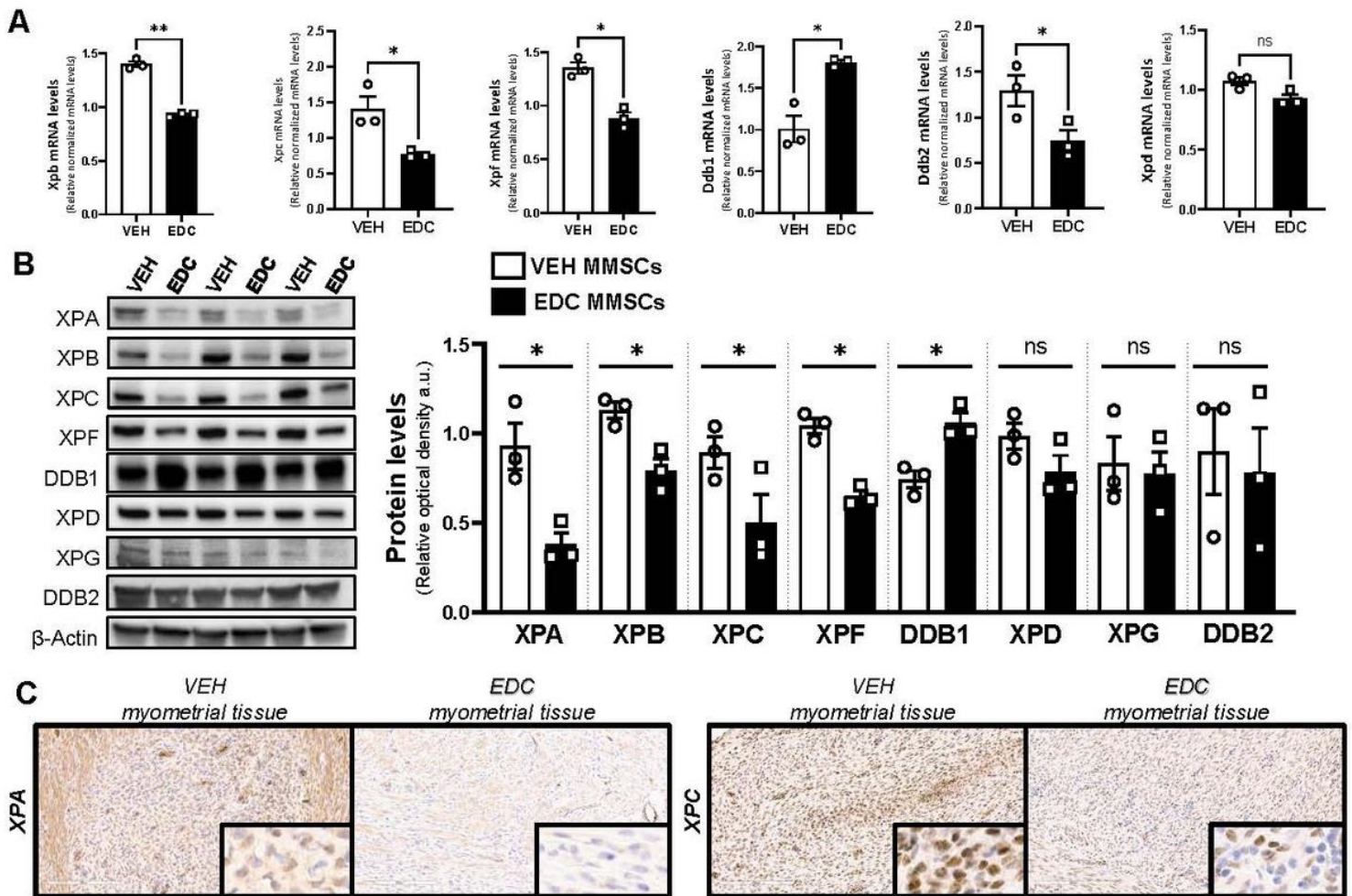


Figure 2

Characterization of nucleotide excision repair (NER) pathway in VEH- and EDC-MMSCs. **A**) mRNA levels of *Xpb*, *Xpc*, *Xpf*, *Ddb1*, *Ddb2* and *Xpd* in VEH- and EDC-MMSCs isolated from 5-months old rats. 18s were used to normalize the expression data. **B**) Representative gel and protein levels of XPA, XPB, XPC, XPF, DDB1, XPD, XPG, and DDB2 in VEH- and EDC- MMSCs isolated from 5-months old rats. Data were normalized by the amount of β-Actin protein levels. **C**) IHC images (20X magnification, insets are at 40X magnification) of XPA and XPC in myometrial tissues from 5-months old Eker rats treated neonatally with VEH or EDC. Scale bar = 200 μm. Data are shown as mean ± S.E.M. from triplicate data. * = p< 0.05, **= p< 0.01, Student's t-test. EDC: endocrine disrupting chemical, MMSCs: myometrial stem cells, XP: Xeroderma pigmentosum, DDB1/2: DNA damage-binding protein 1/2

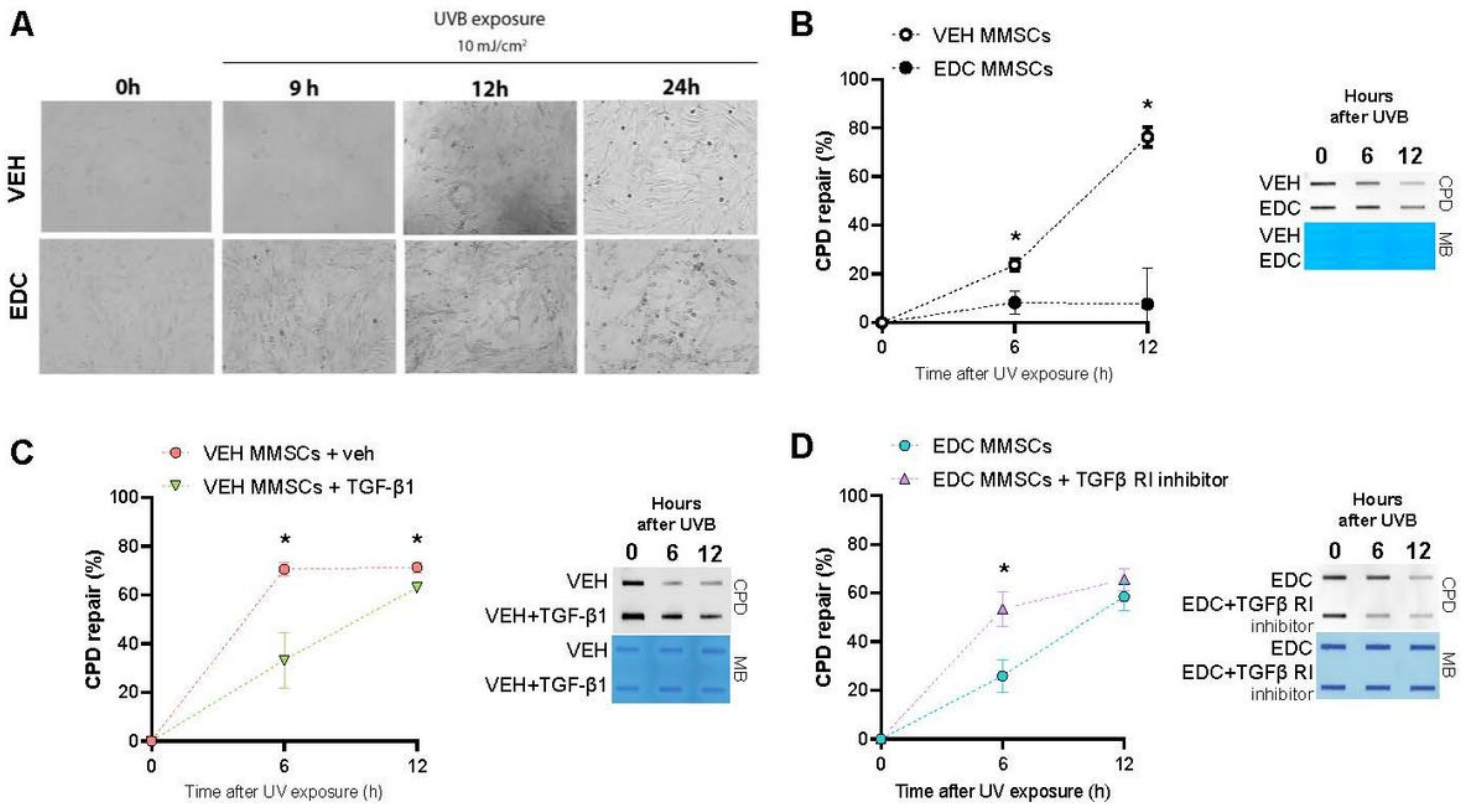


Figure 3

Effect of early life EDC exposure and TGFβ1 on CPD repair. **A)** Bright-field images of VEH- and EDC-MMSCs before (0h) and after UVB exposure (9, 12, and 24 h; 10 mJ/cm²). Magnification 20X. **B)** Quantification of percentage (%) of CPD repair and a representative image of DNA slot blot in VEH- and EDC-MMSCs isolated from 5 months old rats at 0, 6 and 12 h post-UVB (10 mJ/cm²). **C)** Quantification of percentage (%) of CPD repair and a representative image of DNA slot blot in VEH-MMSC treated with vehicle (4 mM HCl + 0.1% BSA) or TGFβ1 (10 ng/ml) for 48 h and then collected at 0, 6 and 12 h post-UVB (10 mJ/cm²). **D)** Quantification of percentage (%) of CPD repair and a representative image of DNA slot blot in EDC-MMSC treated with vehicle (<0.1% DMSO) or TGFβ1 Receptor inhibitor (2μM) for 24 h and then collected at 0, 6 and 12 h post-UVB (10 mJ/cm²). Methylene blue (MB) was used as the loading control. Data are shown as mean ± S.E.M. from triplicate data. *= p < 0.05, Student's t-test

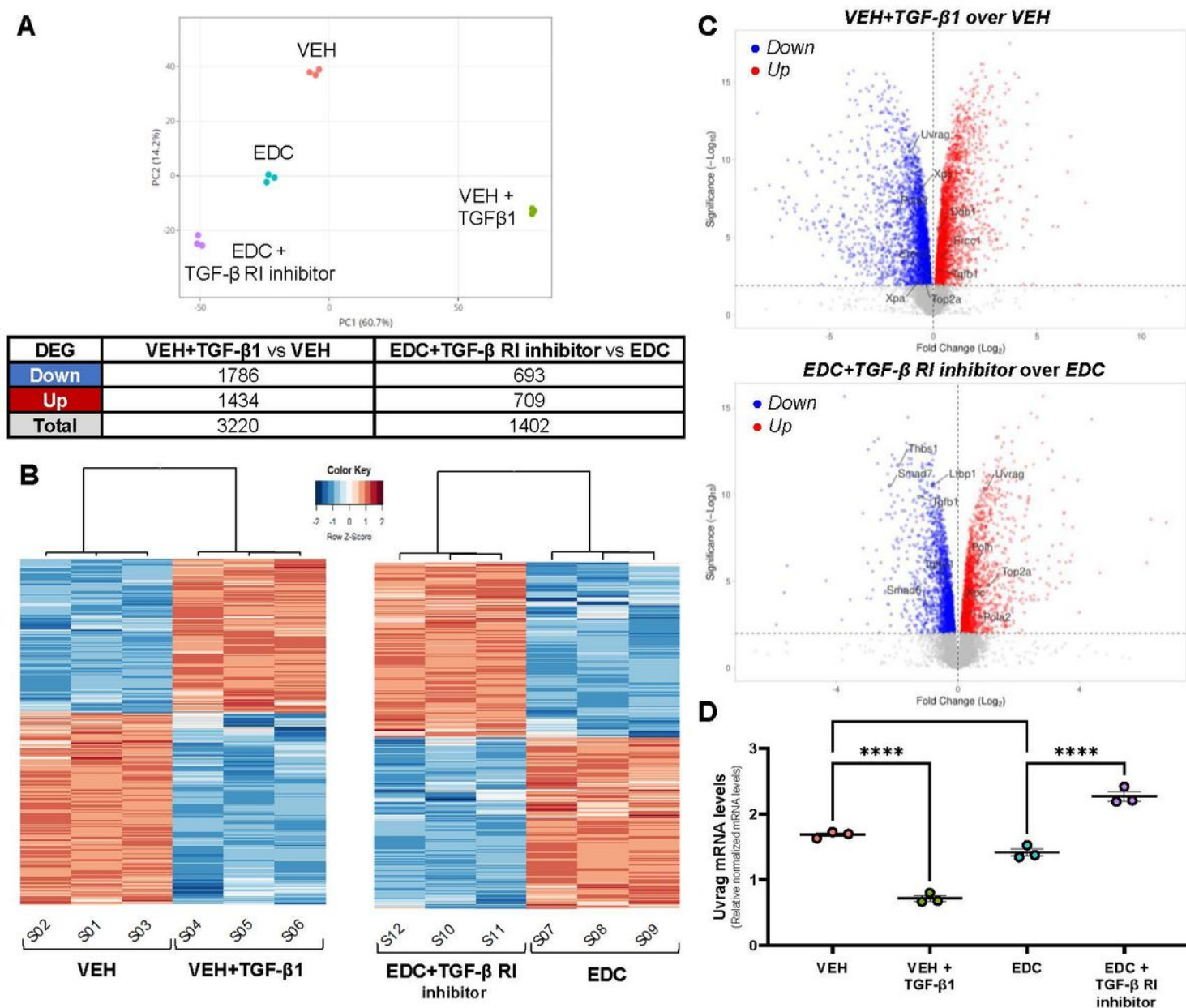


Figure 4

Effect of TGFβ1 pathway activation and inhibition on gene expression of rat VEH- and EDC- MMSCs. **A**) Principal component analysis plot showing samples clustering and DEGs table (Fold change ≥ 1.5 , FDR of 0.05). **B**) Heatmaps representing the DEGs clustered using Pearson correlation in VEH-MMSCs treated with vehicle or TGFβ1 (10 ng/ml) for 48 h (left), and EDC-MMSCs treated with vehicle or TGFβ Receptor I inhibitor (2μM) for 24 h (right). Data is scaled by Z-score for each row. **C**) Volcano plots showing genes downregulated (blue dots) or upregulated (red dots) statistically significant. **D**) mRNA levels of *Uvrag* in VEH MMSCs treated with vehicle or TGFβ1 (10 ng/ml) for 48 h, and EDC MMSCs treated with vehicle or TGFβ Receptor I inhibitor (2μM) for 24 h. *18s* was used to normalize the expression data. Data are shown as mean \pm S.E.M. * = $p < 0.05$, **** = $p < 0.0001$

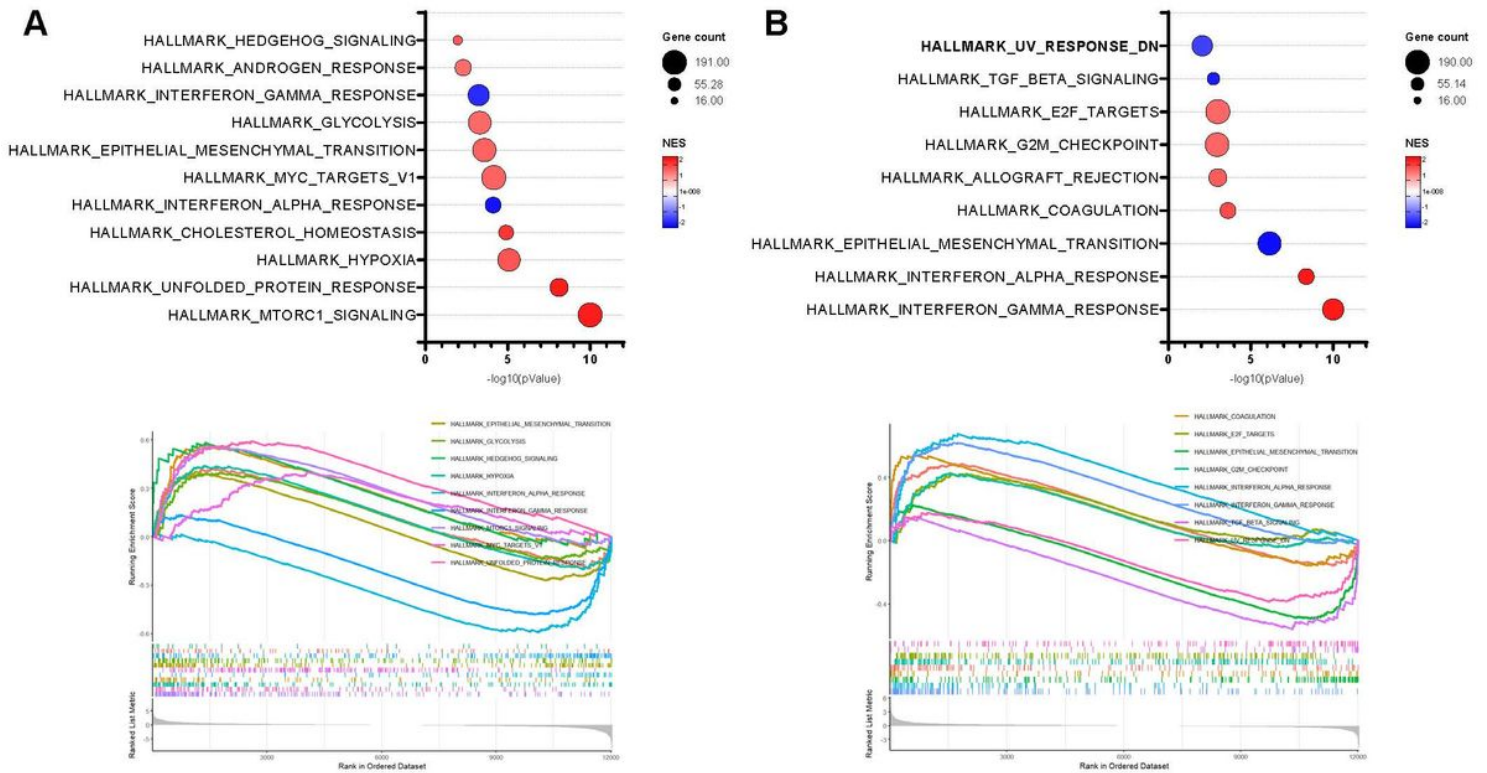


Figure 5

Effect of TGFβ1 pathway activation and inhibition on pathway enrichment of rat VEH- and EDC- MMSCs. A bubble chart of the Gene Set Enrichment Analysis (GSEA) (top) and enrichment plot (bottom) using the Hallmark MSigDB collection for **A**) VEH-MMSCs treated with vehicle or TGFβ1, and **B**) EDC-MMSCs treated with vehicle or TGFβ Receptor I inhibitor comparisons. Normalized enrichment score (NES) is a metric whose sign corresponds to which end of the dataset is enriched in the tested gene set

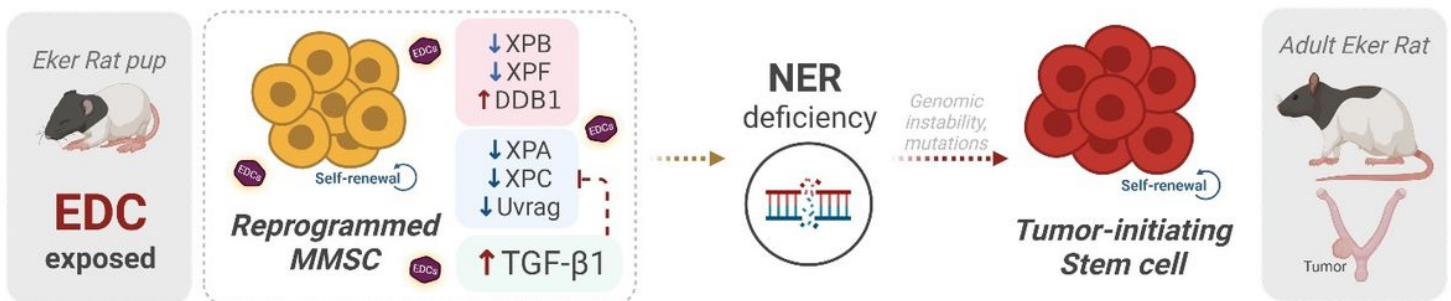


Figure 6

Early life exposure to endocrine-disrupting chemicals reprograms rat MMSC and impaired their capacity to repair the DNA. Myometrial stem cells (MMSC) from Eker rats exposed to endocrine disrupting chemicals (EDCs) in early life present lower levels of several members of nucleotide excision repair (NER) pathway, and overactivation of the TGFβ pathway which is also linked to changes in this DNA damage repair signaling. The reprogrammed

MMSCs present impaired NER capacity, leading to increased genetic instability, arise of mutations, and their transformation into tumor-initiating stem cells, which would result in uterine tumorigenesis later in life. Created with BioRender.com

Supplementary Files

This is a list of supplementary files associated with this preprint. Click to download.

- [SuppFig1.pptx](#)